J. Mater. Environ. Sci. 3 (4) (2012) 613-627 *Rekkab et al.*
ISSN : 2028-2508
CODEN: JMESCN

Green Corrosion Inhibitor from Essential Oil of *Eucalyptus globulus* (Myrtaceae) for C38 Steel in Sulfuric Acid Solution

S. Rekkab [1], H. Zarrok [2], R. Salghi [3,*], A. Zarrouk [4], Lh. Bazzi [5], B. Hammouti [4], Z. Kabouche [1], R. Touzani [4], M. Zougagh [6]

[1] *Laboratory of therapeutics substances (LOST), faculty of sciences, university Mentouri – Constantine, Campus Chaabat Ersas, 25000 Constantine, Algeria*
[2] *Laboratory separation processes, Faculty of Science, University Ibn Tofail PO Box 242, Kenitra, Morocco.*
[3] *Laboratory of Environmental Engineering and Biotechnology, ENSA, University Ibn Zohr, 80000 Agadir, Morocco*
[4] *CAE-URAC 18, Faculty of Science, University of Mohammed Premier, Po Box 717 60000 Oujda, Morocco*
[5] *Laboratory of Establishment of Autonomous Control and Coordination of Export, 80000 Agadir, Morocco*
[6] *Regional Institute for Applied Science Research, IRICA, E-13004 Ciudad Real, Spain*

Received 22 Mar 2012, Revised 1 Apr 2012, Accepted 1 Apr 2012
*Corresponding Author. r_salghi@yahoo.fr, Tel: +(212) 528228313, Fax: +(212) 528232007.

Abstract

The inhibition of the corrosion of C38 steel in sulfuric acid solution by the essential oil of *Eucalyptus globulus* (Myrtaceae) has been studied using weight loss, electrochemical impedance spectroscopy and potentiodynamic polarization techniques. Inhibition was found to increase with increasing concentration of the essential oil. The effect of temperature on the corrosion behavior of C38 steel in 0.5M H_2SO_4 with addition of essential oil was also studied. The adsorption of the essential oil on the C38 steel surface obeyed the Langmuir adsorption isotherm. Values of inhibition efficiency calculated from weight loss, potentiodynamic polarization, and electrochemical impedance spectroscopy are in good agreement. Polarization curves showed that *Eucalyptus globulus* (Myrtaceae) essential oil behaves as a mixed-type inhibitor in sulfuric acid. The activation energy as well as other thermodynamic parameters for the inhibition process was calculated and discussed. The results obtained showed that the essential oil of Eucalyptus globulus (Myrtaceae) could serve as an effective inhibitor of the corrosion of C38 steel in sulfuric acid solution.

Keywords: Eucalyptus globulus (Myrtaceae), C38 Steel, Sulfuric acid, Weight loss, Electrochemical measurement

1. Introduction

Acidic solutions are used in many industrial areas. The most important applications are acid pickling, industrial acid cleaning, acid descaling, and oil well acidizing (1,2). The use of inhibitors is one of the most practical methods for protection against corrosion and prevention of unexpected metal dissolution and acid consumption, especially in acid solutions. Different organic and inorganic compounds have been studied as inhibitors to protect metals from corrosive attack. The efficiency of these organic corrosion inhibitors is related to the presence of polar functions with S, O or N atoms in the molecule, heterocyclic compounds and π-electrons (3). Such compounds can adsorb onto the metal surface and block the active surface sites, thus reducing the corrosion rate. Although many synthetic compound show good anticorrosive activity, most of them are highly toxic to both human beings and the environment (4), and they are often expensive and non-biodegradable. Thus, the use of natural products as corrosion inhibitors has become a key area of research because plant extracts are viewed as an incredibly rich source of naturally synthesized chemical compounds that are biodegradable in nature and can be extracted by simple procedures with low cost (5). The extracts of their leaves (5–14, 16), peels (14–16), seeds (5, 6, 8, 17), fruits (15, 16) and roots (18) have been reported as effective corrosion inhibitors in different aggressive environments. The natural products extracted from leaves have been widely studied as corrosion inhibitors. A large number of scientific studies have been devoted to the inhibitive action of some plant extracts on the corrosion of C-steel in acidic media, showing that these extracts could serve as good corrosion inhibitors; the cited extracts include *Justicia gendarussa* (3), *Lawsonia inermis* (4), *Occimum viridis*, *Telferia occidentalis*, *Azadirachta indica*, *Hibiscus sabdariffa* and *Garcinia kola* (7), *Phyllanthus amarus* (8), *Olea europaea L.* (10), *Ferula harmonis* (18), *Chamaemelum mixtum L.; Cymbopogon proximus*, *Nigella sativa L.* and *Phaseolus vulgares L.* (19), *Zenthoxylum alatum* (20), *Piper nigrum* (21) and *Lupinous albus L.* (22), Shahjan (*Moringa oleifera*), Pipali (*Piper longum*) and Orange (*Citrus aurantium*) [23]. Hammouti et al. studied the extracts of *Ginger* (24), *jojoba oil* (24), eugenol, acetyl-eugenol (25), *artemisia oil* (26), *eucalyptus* oil (27), *Mentha pulegium* (28, 29), *Salvia aucheri Boiss. var. mesatlantica* (30), *Argan oil* (31) and *Mentha Spicata* (32) for corrosion inhibition of steel in acid media.

In continuation of our work on development of green corrosion inhibitors, the present study investigates the inhibiting effect of essential oil of *Eucalyptus globulus* (Myrtaceae). Inhibition effect of *Eucalyptus globulus* (Eu g) on the corrosion of C38 steel in 0.5M H_2SO_4 solution by weight loss, potentiodynamic polarization, and electrochemical impedance spectroscopy (EIS) methods. The effect of temperature is also studied.

2. Experimental

Plant collection and essential oil extraction

Eucalyptus globulus (Myrtaceae) was collected in November 2011 in the region of Constantine (Algeria). A voucher specimen sample was deposited in the herbarium of the laboratory of therapeutics substances (LOST), Faculty of sciences, University Mentouri – Constantine, Algeria.

The fresh cloves of the plant (100 g) were hydrodistilled for 3 hours using a Clevenger-type apparatus recommended by the French Pharmacopoeia (33).

Fatty acid composition

The fatty acid composition was determined following the ISO standard ISO 5509:2000 (ISO 2000) (34). In brief, one drop of the oil was dissolved in 1 mL of n-heptane, 50 µg of sodium methylate was added, and the closed tube was agitated vigorously for 1 min at room temperature. After addition of 100 µL of water, the tube was centrifuged at 4500 × g for 10 min and the lower aqueous phase was removed. Then 50 µL of HCl (1 mol with methyl orange) was added, the solution was shortly mixed, and the lower aqueous phase was rejected. About 20 mg of sodium hydrogen sulphate (monohydrate, extra pure; Merck, Darmstadt, Germany) was added, and after centrifugation at 4500 × g for 10 min, the top n-heptane phase was transferred to a vial and injected in a Agilent Technologies 6890N gas chromatograph equipped with a capillary column (30 m x 0.32 mm; Supelco, Bellefonte, PA, USA) and flame ionization detection. The column was programmed to increase from 135 to 160°C at 2°C/min and from 160 to 205°C at 1.5°C/min; the detection temperature was maintained at 220°C, injector temperature 220 °C. The vector gas was helium at a pressure of 5520 Pa. Peaks were identified by comparing retention times with those of standard fatty acid methyl esters.

Weight loss measurements

Coupons were cut into 2 × 2 × 0.08 cm^3 dimensions having composition (0.179% C, 0.165% Si, 0.439% Mn, 0.203% Cu, 0.034% S and Fe balance) are used for weight loss measurements. Prior to all measurements, the exposed area was mechanically abraded with 180, 320, 800, 1200 grades of emery papers. The specimens are washed thoroughly with bidistilled water, degreased and dried with ethanol. Gravimetric measurements are carried out in a double walled glass cell equipped with a thermostated cooling condenser. The solution volume is 80 cm^3. The immersion time for the weight loss is 6 h at 298 K.

Electrochemical tests

The electrochemical study was carried out using a potentiostat PGZ100 piloted by Voltamaster software. This potentiostat is connected to a cell with three electrode thermostats with double wall (Tacussel Standard CEC/TH). A saturated calomel electrode (SCE) and platinum electrode were used as reference and auxiliary electrodes, respectively. The material used for constructing the working electrode was the same used for gravimetric measurements. The surface area exposed to the electrolyte is 0.056 cm^2.

Potentiodynamic polarization curves were plotted at a polarization scan rate of 0.5 mV/s. Before all experiments, the potential was stabilized at free potential during 30 min. The polarisation curves are obtained from −800 mV to −400 mV at 298 K. The solution test is there after de-aerated by bubbling nitrogen. Gas bubbling is maintained prior and through the experiments. In order to investigate the effects of temperature and immersion time on the inhibitor performance, some test were carried out in a temperature range 298–328 K.

The electrochemical impedance spectroscopy (EIS) measurements are carried out with the electrochemical system (Tacussel), which included a digital potentiostat model Voltalab PGZ100 computer at E_{corr} after immersion in solution without bubbling. After the determination of steady-state current at a corrosion potential, sine wave voltage (10 mV) peak to peak, at frequencies between 100 kHz and 10 mHz are superimposed on the rest potential. Computer programs automatically controlled the measurements performed at rest potentials after 0.5 hour of exposure at 298 K. The impedance diagrams are given in the Nyquist representation. Experiments are repeated three times to ensure the reproducibility.

Solutions preparation

The solution 0.5M H_2SO_4 was prepared by dilution of analytical grade 98% H_2SO_4 with double distilled water. The solution tests are freshly prepared before each experiment by adding the oil directly to the corrosive solution. The test solutions were freshly prepared before each experiment by adding the oil directly to the corrosive solution. The test solution is there after de-aerated by bubbling nitrogen. Gas pebbling is maintained prior and through the experiments. Experiments were carried out in triplicate to ensure the reproducibility.

3 Results and Discussion

Fatty acid composition

The yield was determined as grams over the 100 g of powder analyzed in percentage, and is shown in Table 1.

Table 1. Fatty acid compositions of *Eucalyptus* oil (%).

Plant species	Family	Yield (%) A	Major constituents	(%) B
Eucalyptus	Myrtaceae	2 gr	Pentadecanoic acid	01.90
			Palmitic acid	36.00
			Palmitoleic acid	07.30
			Margaric acid	00.70
			Heptadecenoic acid	01.00
			Stearic acid	03.30
			Oleic acid	27.20
			Linoleic acid	19.30

A: Grams of essential oiled oil as percentage over the 100 g of powder analysed.
B: Grams over total essential oiled oil in percentage.

Potentiodynamic polarization measurements

The typical Tafel polarization curves of C38 steel in 0.5M H_2SO_4 in the presence and absence of *Eucalyptus globulus* (Myrtaceae) at different concentrations are shown in Figure 1. It could be observed that both the cathodic and anodic reactions were suppressed with the addition of *Eucalyptus globulus* (Myrtaceae), which suggests that the *Eucalyptus globulus* (Myrtaceae) reduced anodic dissolution and also retarded the hydrogen evolution reaction effectively.

Various corrosion kinetics parameters, i.e. corrosion potential (E_{corr}), cathodic Tafel slope (β_c) and corrosion current density (I_{corr}) obtained from the Tafel extrapolation of the polarization curves, are given in Table 2. The ($E_I(\%)$) is calculated using the following equation (35):

$$E_I(\%) = \left(\frac{I_{corr} - I'_{corr}}{I_{corr}}\right) \times 100 \quad (1)$$

Where I_{corr} and I'_{corr} are uninhibited and inhibited corrosion current densities, respectively. Under the experimental conditions performed, the cathodic branch represents the hydrogen evolution reaction, while the anodic branch represents the iron dissolution reaction. They are determined by extrapolation of Tafel lines to the respective corrosion potentials. Some of the authors proposed the following mechanism for the corrosion of iron and steel in acid solution (36–38):

$$Fe + A^{n-} \rightarrow (FeA^{n+})_{ads}$$

$$(FeA^{n-})_{ads} \rightarrow (FeA^{n-})_{ads} + ne^-$$

$$(FeA^{n-})_{ads} \rightarrow (FeA^{n+})_{ads} + ne^-$$

$$(FeA^{n+})_{ads} \rightarrow (Fe^{2+})_{ads} + A^{n-}$$

The cathodic hydrogen evolution

$$Fe + H^+ \rightarrow (FeH^+)_{ads}$$

$$(FeH^+)_{ads} + ne^- \rightarrow (FeH)_{ads}$$

$$(FeH^+)_{ads} + H^+ + ne^- \rightarrow Fe + H_2$$

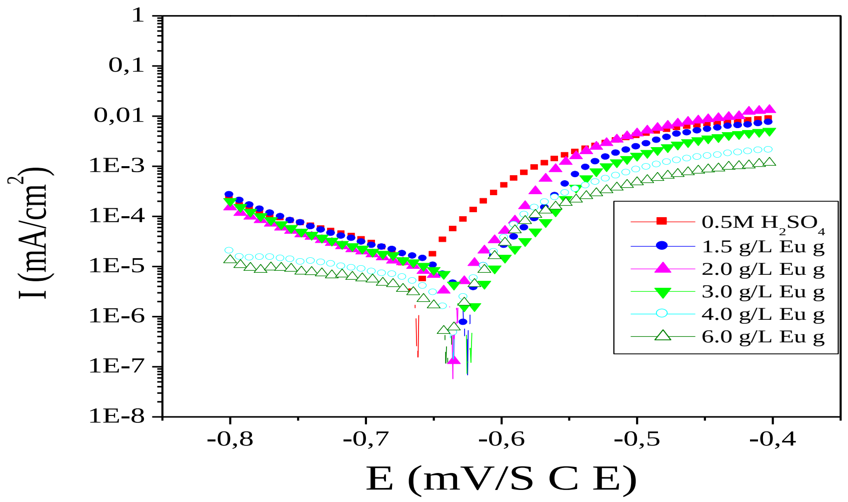

Figure 1. Polarization curves in the absence and presence of different concentrations of essential oil in 0.5M H_2SO_4

Table 2. Electrochemical parameters of C38 steel at various concentrations of essential oil studied in 0.5M H_2SO_4 at 298 K.

Inhibitor	Conc	$-E_{corr}$ (mV/SCE)	$-\beta_c$ (mV/dec)	I_{corr} ($\mu A/cm^2$)	E_I (%)
H_2SO_4	0.5 M	662.9	141.8	17.9	-
Eu g	1.5 g/L	628.6	100.7	07.1	60.3
	2.0 g/L	633.0	105.5	06.3	64.8
	3.0 g/L	624.3	92.5	05.7	68.2
	4.0 g/L	636.5	126.2	04.6	74.3
	6.0 g/L	639.8	145.7	03.4	**81.0**

Inspection of this result reveals that in presence of inhibitor, the value of corrosion density (I_{corr}) was decreased. This behavior reflects its ability to inhibit the corrosion of C38 steel in 0.5M H_2SO_4 solution. Both the anodic and cathodic current densities were decreased in Fig. 1 indicating that *Eucalyptus globulus* (Myrtaceae) suppressed both the anodic and cathodic reactions through adsorption on the C38 steel surface. This suggests that *Eucalyptus globulus* (Myrtaceae) act as mixed type corrosion inhibitor for C38 steel in 0.5M H_2SO_4 solution (39). Generaly, the modes of the inhibition effect of inhibitors are classified into three categories (40-42): geometric blocking effect of adsorbed inhibitive species, active sites blocking effect by adsorbed inhibitive species, and electro-catalytic effect of the inhibitor or its reaction products. It has been discussed in the case of the first mode that inhibition effect comes from the reduction of the reaction area on the surface of the corroding metal, whereas for the other two modes the inhibition effects are due to the changes in the average activation energy barriers of the anodic and cathodic reactions of the corrosion process. Cao (42) explained that if the shift of corrosion potential due to addition of an interface inhibitor is negligible, the inhibition is most probably caused by a geometric blocking effect of the adsorbed inhibitive species on the surface corroding metal. The cathodic Tafel slope (β_c) show slight changes with the addition of *Eucalyptus globulus* (Myrtaceae), which suggests that the inhibiting action occurred by simple blocking of the available cathodic sites on the metal surface, which lead to a decrease in the exposed area necessary for hydrogen evolution and lowered the dissolution rate with increasing *Eucalyptus globulus* (Myrtaceae) concentration. The parallel cathodic Tafel plots obtained in Figure 1 indicate that the hydrogen evolution is activation-controlled and the reduction mechanism is not affected by the presence of inhibitor (43).

Electrochemical impedance measurements

The corrosion behaviour of C38 steel in 0.5M H_2SO_4 solution, in the absence and presence of *Eucalyptus globulus* (Myrtaceae), is also investigated by the EIS at 298 K after 30 min of immersion. The charge-transfer resistance values were obtained from the diameter of the semicircles of the Nyquist plots. The inhibition efficiency of the inhibitor has been found out from the charge transfer resistance values using the following equation:

$$E_{R_{ct}} \% = \frac{R_{ct} - R^{0}_{ct}}{R_{ct}} \times 100 \qquad (2)$$

Where, R^{0}_{ct} and R_{ct} are the charge transfer resistance in absence and in presence of inhibitor, respectively. All electrochemical measurements were done in unstirred and non-de-aerated solutions.

The electrochemical impedance diagrams for C38 steel in 0.5M H_2SO_4 solution in the absence and presence of various concentrations of aqueous essential oil from *Eucalyptus globulus* (Myrtaceae) are shown in Figure 2. Table 3 summarizes impedance data from the EIS experiments carried out both in the absence and presence of increasing essential oil concentrations.

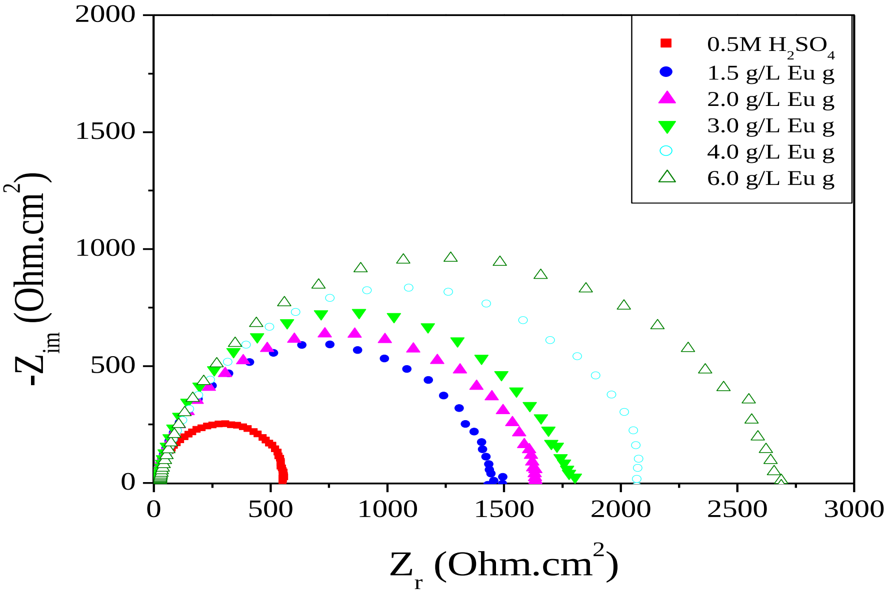

Figure 2. Nyquist plots in absence and presence of different concentrations of essential oil in 0.5M H_2SO_4

Table 3. Corrosion parameters obtained by impedance measurements for C38 steel in 0.5M H_2SO_4 at various concentrations of essential oil.

Inhibitor	Conc	R_{ct} (Ω.cm^2)	f_{max} (Hz)	C_{dl} (μF/cm^2)	E_{Rct} (%)
H_2SO_4	0.5 M	560.2	63.33	4.488	-
Eu g	1.5 g/L	1473.0	40	2.700	62.0
	2.0 g/L	1632.0	40	2.427	65.7
	3.0 g/L	1811.0	40	2.198	69.1
	4.0 g/L	2008.0	40	1.982	72.1
	6.0 g/L	2625.0	31.65	1.915	**78.7**

The electrochemical impedance diagrams show only one depressed capacitive loop, which is attributed to the one time constant, in the absence and presence of the *Eucalyptus globulus* essential oil, which indicates two significant effects: the charge-transfer resistance significantly increases, and the f_{max} decreases, in the presence of the essential oil, decreasing the capacitance value, which may be caused by reduction in the local dielectric constant and/or by an increase in the thickness of the electrical double-layer. These results show that the presence of the essential oils modifies the electric double-layer structure suggesting that the inhibitor molecules act by adsorption at the metal/solution interface. Furthermore, C_{dl} decreases with increase of the concentration of inhibitor (Figure 3). This phenomenon is generally related to the adsorption of organic molecules on the metal surface and then leads to a decrease in the local dielectric constant and/or an increase in the thickness of the electrical double layer (44).

$$C_{dl} = \frac{\varepsilon_o \varepsilon}{\delta} S \qquad (4)$$

Where δ is the thickness of the protective layer, S is the electrode area, ε_o the vacuum permittivity of vide and ε is dielectric constant of the medium.

A low capacitance may result if water molecules at the electrode interface are largely replaced by organic inhibitor molecules through adsorption (45). The larger inhibitor molecules also reduce the capacitance through the increase in the double layer thickness (46). Deviations from a perfect circular shape indicate frequency dispersion of interfacial impedance. This anomalous phenomenon is attributed in the literature to the non homogeneity of the electrode surface arising from the surface roughness or interfacial phenomena (4, 16, 21, 22, 28, 47). The charge-transfer resistance (R_{ct}) values were calculated from the difference in impedances at lower and higher frequencies. The double-layer capacitance (C_{dl}) was calculated from the following equation:

$$C_{dl} = \frac{1}{2\pi f_{\max} R_{ct}} \qquad (3)$$

where f_{max} is the frequency at which the imaginary component of the impedance is maximal. A C_{dl} value of 4.488 µF cm^{-2} was found for the C38 steel electrode at 0.5M H_2SO_4.

From Table 3, it is clear that the R_{ct} values increased and that the C_{dl} values decreased with increasing inhibitor concentration. This result indicates a decrease in the active surface area caused by the adsorption of the inhibitor on the carbon steel surface, and it suggests that the corrosion process became hindered; this hypothesis is corroborated by the anodic and cathodic polarization curves and the corrosion potential results. The best result for the inhibition efficiency of this essential oil was obtained at a concentration of 6 g L^{-1}, with efficiency equal to 79%.

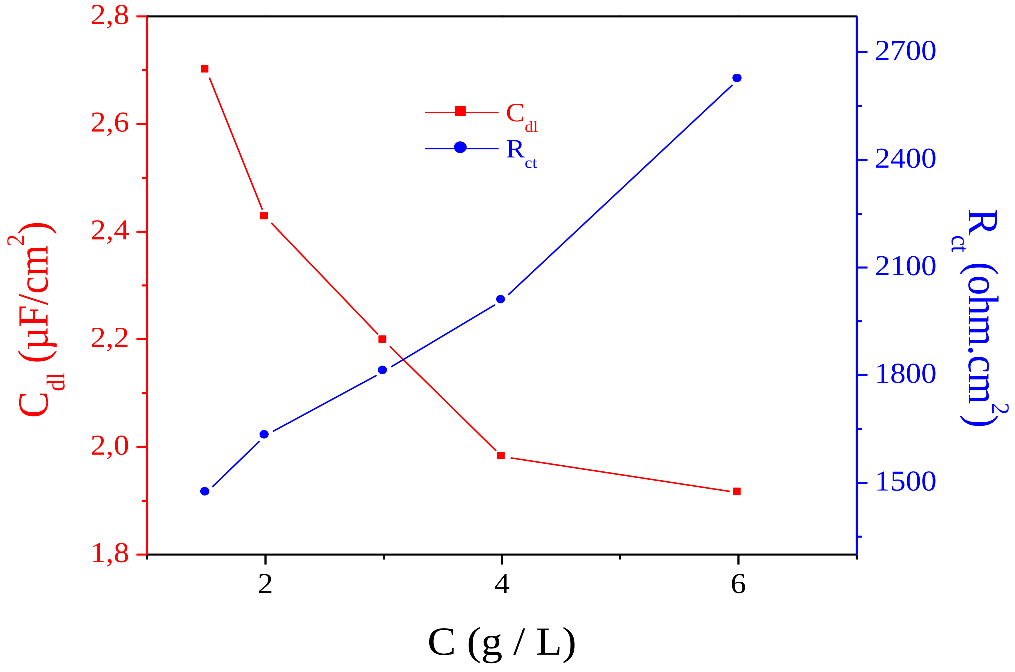

Figure 3. Evolution of transfer resistance and capacitance as function of essential oil concentration.

Weight loss measurements

3.4.1. Effect of Inhibitor concentration

Weight loss data of C38 steel in 0.5M H_2SO_4 in the absence and presence of various concentrations of inhibitor were obtained and are given in Table 4. From the weight loss results, the inhibition efficiency (E_w%) of the inhibitor and degree of surface coverage (Θ) were calculated using equations 4 and 5 (48);

$$E_w\% = \left(1 - \frac{W_{corr}}{W^{\circ}_{corr}}\right) \times 100 \qquad (4)$$

$$\Theta = 1 - \frac{W_{corr}}{W^{0}_{corr}} \qquad (5)$$

Where W_{corr} and W^{o}_{corr} are the weight losses for C38 steel in the presence and absence of the essential oil in H_2SO_4 solution and Θ is the degree of surface coverage of the inhibitor.

Figure 4 illustrates the variation of corrosion rate and efficiencies with concentration of inhibitor. It has been found off this compound inhibit the corrosion of C38 steel in H_2SO_4 solution at all concentrations used in this study. It has also been observed that the inhibition efficiency for this compound increases with the increase in concentration. Maximum E_w (%) for this compound was achieved at 6 g L^{-1} and a further increase in concentration did not cause any appreciable change in the performance of the inhibitor (gravimetric measurement). The corrosion inhibition can be attributed to the adsorption of this compound at the C38 steel / acid solution interface. The corrosion rate decreases with the concentration of inhibitor and in turn the inhibition efficiency evaluated from weight loss measurements for this compound increases to attain 75.8 % for 6 g L^{-1}.

Table 4. Weight loss results for C38 steel in 0.5M H_2SO_4 in the absence and presence of essential oil at various concentrations.

Inhibitor	Conc	CR (mg/cm^2.h)	E_w (%)	Θ
H_2SO_4	0.5 M	1.789	-	-
	1.5 g/L	0.723	59.6	0.5959
	2.0 g/L	0.640	64.2	0.6423
Eucalyptus	3.0 g/L	0.597	66.6	0.6663
	4.0 g/L	0.515	71.2	0.7121
	5.0 g/L	0.507	71.7	0.7166
	6.0 g/L	0.433	75.8	0.7580

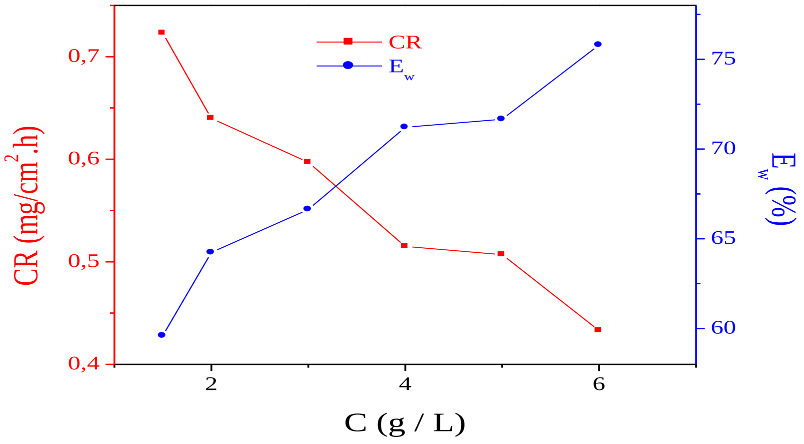

Figure 4. Variation of the corrosion rate and inhibitive efficiency against the essential oil concentrations.

A comparison may be made between inhibition efficiency *E* (%) values obtained by different methods (weight loss, polarisation curves and EIS methods). Figure 5 shows a curve that compares the *E* (%) values obtained. One can see that whatever the method used, no significant changes are observed in *E* (%) values. We can then conclude that there is a good correlation with the three methods used in this investigation at all tested concentrations and that *Eucalyptus globulus* is an efficient corrosion inhibitor.

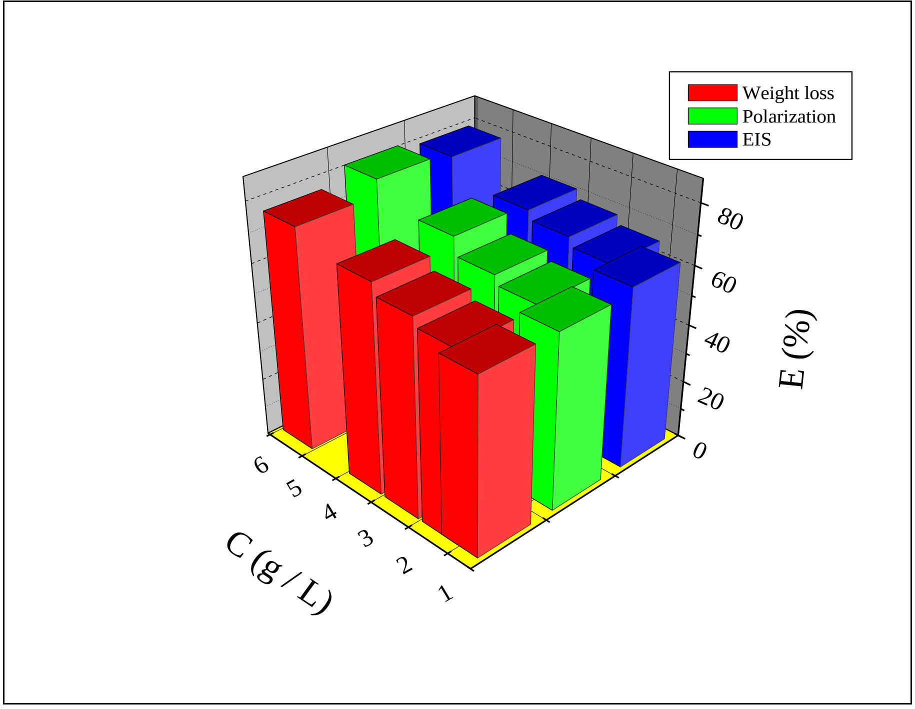

Figure 5. Comparison of inhibition efficiency (E %) values obtained by weight loss,polarisation and EIS methods

Effect of temperature

In order to study the effect of temperature on the inhibition efficiencies of *Eucalyptus globulus* essential oil, weight loss measurements were carried out in the temperature range (298–328K) during 1 hour of immersion in absence and presence of inhibitor at optimum concentration. The various corrosion parameters obtained are listed in Table 5. Figure 6 illustrates the variation of corrosion rate in the absence and of inhibitor at optimum concentration at different temperatures.

Table 5. Various corrosion parameters for C38 steel in 0.5M H_2SO_4 in absence and presence of optimum concentration of essential oil at different temperatures

Temperature (K)	Inhibitor	CR(mg/cm^2.h)	E_w (%)	Θ
298	Blank	1.791	-	-
	Eu g	0.430	76	0.76
308	Blank	3.154	-	-
	Eu g	1.009	68	0.68
318	Blank	4.704	-	-
	Eu g	2.446	48	0.48
328	Blank	7.696	-	-
	Eu g	4.156	46	0.46

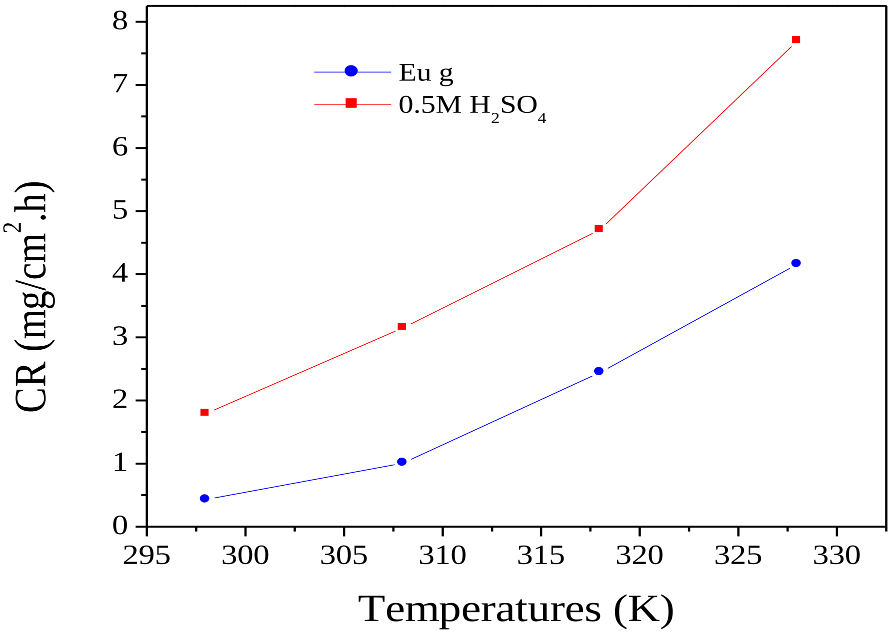

Figure 6. Variation of corrosion rate in 0.5M H_2SO_4 on steel surface without and with of optimum concentration of essential oil at different temperatures.

The fractional surface coverage Θ can be easily determined from the weight loss measurements by the ratio E% /100, where E % is inhibition efficiency and calculated using relation 5. The data obtained suggest that essential oil get adsorbed on the steel surface at all temperatures studied and corrosion rates increased in absence and presence of inhibitor with increase in temperature in 0.5M H_2SO_4 solutions. In acidic media, corrosion of metal is generally accompanied with evolution of H_2 gas; rise in temperature usually accelerates the corrosion reactions which results in higher dissolution rate of the metal. Inspection of Table 5 showed that corrosion rate increased with increasing temperature both in uninhibited and inhibited solutions while the inhibition efficiency of essential oil decreased with temperature. A decrease in inhibition efficiencies with the increase temperature in presence of essential oil might be due to weakening of physical adsorption.

In order to calculate activation parameters for the corrosion process, Arrhenius Eq. (5) and transition state Eq. (6) were used (49):

$$C_R = A\exp\left(\frac{-E_a}{RT}\right) \quad (5)$$

$$C_R = \frac{RT}{Nh}\exp\left(\frac{\Delta S_a^*}{R}\right)\exp\left(-\frac{\Delta H_a^*}{RT}\right) \quad (6)$$

Where C_R is the corrosion rate, R the gas constant, T the absolute temperature, A the pre-exponential factor, h the Plank's constant and N is Avogrado's number, E_a the activation energy for corrosion process , ΔH_a^* the enthalpy of activation and ΔS_a^* the entropy of activation.

The apparent activation energie (E_a) at optimum concentration of essential oil was determined by linear regression between Ln C_R and 1/T (Figure 7) and the result is shown in Table 6. The linear regression coefficient was close to 1, indicating that the steel corrosion in sulfuric acid can be elucidated using the kinetic model. Inspection of Table 6 showed that the value of E_a determined in 0.5M H_2SO_4 containing essential oil is higher (62.63 kJ mol^{-1}) than that for uninhibited solution (38.81 kJ mol^{-1}). The increase in the apparent activation energy may be interpreted as physical adsorption that occurs in the first stage (50). Szauer and Brand explained that the increase in activation energy can be attributed to an appreciable decrease in the adsorption of the inhibitor on the steel surface with increase in temperature. As adsorption decreases more desorption of inhibitor occur because these two opposite processes are in equilibrium. Due to more desorption of inhibitor molecules at higher temperatures the greater surface area of steel comes in contact with aggressive environment, resulting increased corrosion rates with increase in temperature (51).

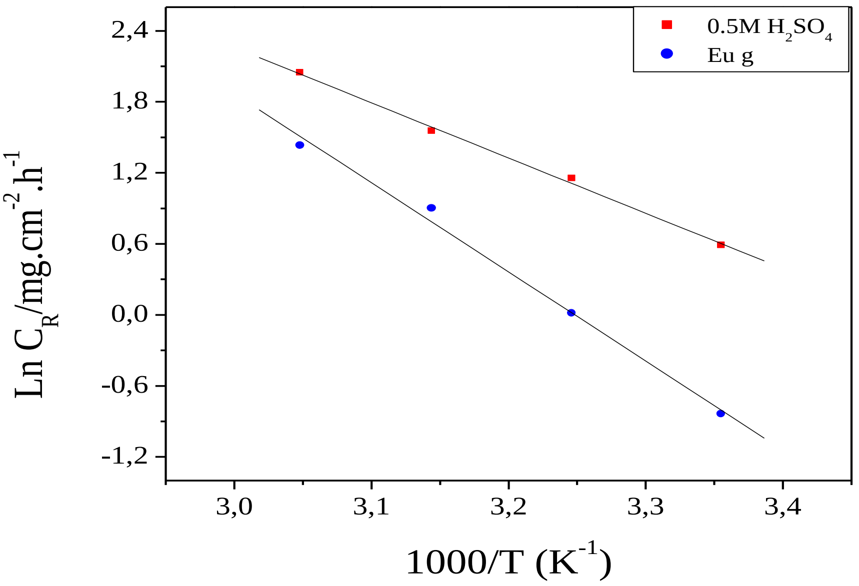

Figure 7. Arrhenius plots of log C_R vs. 1/T for steel in 0.5M H_2SO_4 in the absence and the presence of essential oil at optimum concentration.

Figure 8 showed a plot of Ln (C_R/T) versus 1/T. The straight lines are obtained with a slope (ΔH_a^* /R) and an intercept of (Ln R/Nh + ΔS^*_a /R) from which the values of the values of ΔH_a^* and ΔS_a^* are calculated and are given in Table 6. Inspection of these data revealed that the thermodynamic parameter (ΔH_a^*) for dissolution reaction of steel in 0.5M H_2SO_4 in the presence of essential oil is higher (60.03 kJ mol^{-1}) than that of in the absence of inhibitors (36.21 kJ mol^{-1}). The positive sign of ΔH_a^* reflect the endothermic nature of the steel dissolution process suggesting that the dissolution of steel is slow (52) in the presence of inhibitor.

Table 6. Activation parameters E_a, ΔH_a^* and ΔS_a^* for the C38 steel dissolution in 0.5M H_2SO_4 in the absence and the presence of essential oil at optimum concentration.

	A (mg/cm^2.h)	Linear regression coefficient (r)	E_a (kJ/mol)	ΔH_a° (kJ/mol)	ΔS_a° (J/mol.K)
Blank	1.155×10^7	0,99855	38.81	36.21	-118.42
Eu g	4.232×10^{10}	0,9966	62.63	60.03	-50.19

Large and negative value of entropie (ΔS_a^*) imply that the activated complex in the rate determining step represents an association rather than a dissociation step, meaning that a decrease in disordering takes place on going from reactant to the activated complex (53, 54).

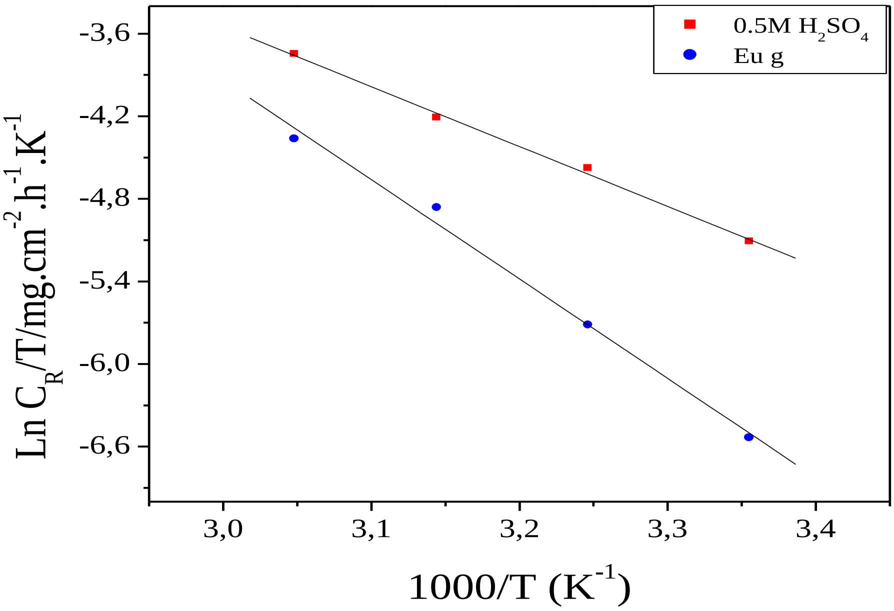

Figure 8. Arrhenius plots of log C_R/T vs. 1/T for steel in 0.5M H_2SO_4 in the absence and the presence of essential oil at optimum concentration.

Adsorption isotherm

It is well established that the first step in corrosion inhibition of metals and alloys is the adsorption of organic inhibitor molecules at the metal/solution interface and that the adsorption depends on the molecule's chemical composition, the temperature and the electrochemical potential at the metal/solution interface. In fact, the solvent water molecules could also adsorb at metal/solution interface. So the adsorption of organic inhibitor molecules from the aqueous solution can be regarded as a quasi-substitution process between the organic compounds in the aqueous phase [Org(sol)] and water molecules at the electrode surface [H_2O(ads)] (55).

$$\mathrm{Org}_{(sol)} + n\mathrm{H_2O}_{(ads)} \Leftrightarrow \mathrm{Org}_{(ads)} + n\mathrm{H_2O}_{(sol)}$$

where Org(sol) and Org(ads) are the organic specie dissolved in the aqueous solution and adsorbed onto the metallic surface, respectively, H_2O(ads) is the water molecule adsorbed on the metallic surface and n is the size ratio representing the number of water molecules replaced by one organic adsorbate. Basic information on the adsorption of inhibitors on the metal surface can be provided by adsorption isotherm. In order to obtain the isotherm, the fractional surface coverage values (Θ) as a function of inhibitor concentration must be obtained. The values of Θ can be easily determined from the weight loss measurements by the ratio E_W%/100, where E_W% is inhibition efficiency obtained by weight loss method. So it is necessary to determine empirically which isotherm fits best to the adsorption of inhibitors on the steel surface. Several adsorption isotherms (viz.; Frumkin, Langmuir, Temkin, Freundlich) were tested and the Langmuir adsorption isotherm was found to provide the best description of the adsorption behaviour of this inhibitor. The Langmuir isotherm is given by following equation (56):

$$\frac{\Theta}{1-\Theta} = K_{ads} C_{inh} \quad (6)$$

The rearrangement gives the following equation : $\frac{C_{inh}}{\Theta} = \frac{1}{K_{ads}} + C_{inh}$ (7)

Where C_{inh} is the concentration of inhibitor, K_{ads} is the equilibrium constant of the adsorption process, and Θ is the surface coverage.

Plot C_{inh}/Θ versus C_{inh} yield a straight line (Figure 9) with regression coefficient, R^2, almost equal to 1. This suggests that exract in present study obeyed the Langmuir isotherm and there is negligible interaction between the adsorbed molecules. Free energy of adsorption was calculated using the relation (57):

$$K_{ads} = \frac{1}{55.55} \exp\left(-\frac{\Delta G^{\circ}_{ads}}{RT}\right) \quad (8)$$

Where R is the universal gas constant and T is the absolute temperature. The value 55.55 in the above equation is the concentration of water in solution in mol L^{-1}.

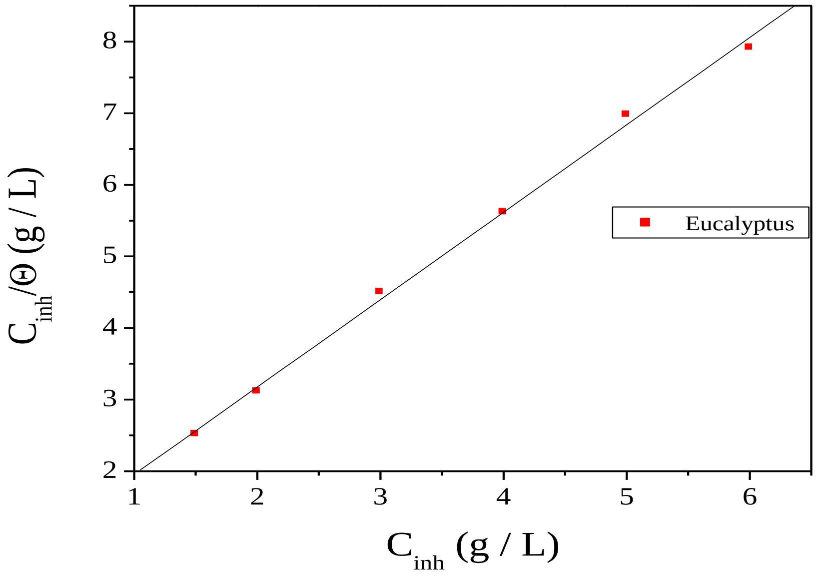

Figure 9. Langmuir adsorption isotherm of *Eucalyptus* oil on the steel surface.

On the basis of characterization of Eucalyptus essential oil, we postulate that the major components act together by adsorption to ensure inhibition. Then, the inhibition is regarded as intermolecular synergistic effect of the various components of natural oil or essential oil (58-60). It is adequately recommended to not determine ΔG_{ads} values since the mechanism of adsorption remains unknown [60].

Conclusions

In this work, we have studied the behaviour of corrosion of C38 steel corrosion in sulfuric acid taking account the effect of the addition of *Eucalyptus globulus* (Myrtaceae) at different concentrations by potentiodynamic polarisation, electrochemical impedance spectroscopy (EIS) and weight loss measurements. From the obtained results, we can have the following conclusions:

1. Results obtained from the experimental and theoretical data show that *Eucalyptus globulus* (Myrtaceae) acts as an effective inhibitor of C38 steel corrosion in sulfuric acid.

2. The corrosion process was inhibited by adsorption of the organic matter on the C38 steel surface.
3. Inhibition efficiency Increases with increase in the concentration of the *Eucalyptus globulus* but decreases with rise in temperature.
4. The adsorption of *Eucalyptus globulus* on C38 steel surface from 0.5M H_2SO_4 obeys the Langmuir adsorption isotherm.
5. The negative values of ΔG°_{ads} indicate that the adsorption of the essential oil is a spontaneous process and an adsorption mechanism is typical of physisorption.
6. Polarisation measurements show that *Eucalyptus globulus* acts essentially as a mixed type inhibitor.
7. The inhibitor efficiencie determined by electrochemical polarisation, electrochemical impedance spectroscopy and by gravimetric methods are in good agreement.

References

(1) Chebabe, D.; Ait Chikh, Z.; Hajjaji, N. *Corros. Sci*. **2003**, 45, 309-320.
(2) Khaled, K. F.; Hackerman, N. *Mater. Chem. Phys*. **2003**, 82, 949-960.
(3) Barouni, K.; Bazzi, L.; Salghi, R.; Mihit, M.; Hammouti, B.; Albourine, A.; El Issami, S. *Materials Letters*. **2008**, 62, 3325-3327.
(4) Ostovari, A.; Hoseinieh, S. M.; Peikari, M.; Shadizadeh, S. R.; Hashemi, S. J. *Corros. Sci*. **2009**, 51, 1935-1949.
(5) Abiola, O. K.; Otaigbe, J. O. E.; Kio, O. J. *Corros. Sci*. **2009**, 51, 1879-1881.
(6) Abiola, O. K.; Otaigbe, J. O. E. *Corros. Sci*. **2009**, 51, 2790-2793.
(7) Oguzie, E. E. *Corros. Sci*. **2008**, 50, 2993-2998.
(8) Okafor, P. C.; Ikpi, M. E.; Uwaha, I. E.; Ebenso, E. E.; Ekpe, U. J.; Umoren, S. A. *Corros. Sci*. **2008**, 50, 2310-2317.
(9) El-Etre, A. Y.; Abdallah, M.; El-Tantawy, Z. E. *Corros. Sci*. **2005**. 47, 385-395.
(10) El-Etre, A. Y. J. *Colloid Interface Sci*. **2007**, 314, 578-583.
(11) Valek, L.; Martinez, S. *Mater. Lett*. **2007**, 61, 148-151.
(12) Oguzie E. E. *Corros. Sci*. **2007**, 49, 1527-1539.
(13) Abiola, O. K.; James, A. O. *Corros*. Sci. *2010*, 52, 661-664.
(14) Loto, C. A. *Corros. Prev Control*. **2001**, 48, 59-64.
(15) Loto, C. A. *Corros. Prev. Control*. **2001**. 48, 38-41.
(16) Quraishi, M. A.; Farooqi, I. H.; Saini, P. A. *Corrosion*. **1999**, 55, 493-497.
(17) El-Etre, A. Y. *Appl. Surf. Sci*. **2006**, 252, 8521-8525.
(18) El-Etre, A. Y. Mater. *Chem. Phys*. **2008**, 108, 278-282.
(19) Abdel-Gaber, A. M.; Abd-El-Nabey, B. A.; Sidahmed, I. M.; El-Zayady, A. M.; Saadawy, M. *Corros. Sci*. **2006**, 48, 2765-2779.
(20) Chauhan, L. R.; Gunasekaran, G. *Corros. Sci*. **2007**, 49, 1143-1161.
(21) Raja, P. B.; Sethuraman, M. G. *Mater. Lett.* **2008**, 62, 2977-2979.
(22) Abdel-Gaber, A. M.; Abd-El-Nabey, B. A.; Saadawy, M. *Corros. Sci*. **2009**, 51, 1038-1042.
(23) Ambrish, S.; Singh, V. K.; Quraishi, M. A. *J. Mater. Environ. Sci*. **2010**, 1, 162-174
(24) Bouyanzer, A.; Hammouti B. *Bull. Electrochem*. **2004**, 20, 63-65.
(25) Chetouani, A.; Hammouti B.; Benkaddour M. *Pigm. Res. Technol*. **2004**, 33, 26-31.
(26) Chaieb, E A.; Bouyanzer, A.; Hammouti ,B.; Benkaddour, M. *Appl. Surf. Sci*. **2005**, 246, 199-206.
(27) Bouyanzer, A.; Majidi L.; Hammouti, B. *Bull. Electrochem*. **2006**, 22, 321-324.
(28) Benabdellah, M.; Benkaddour, M.; Hammouti, B.; Bendahhou, M.; Aouniti, A. *Appl. Surf. Sci*. **2006**, 252, 6212-6217.
(29) Bouyanzer, A.; Hammouti, B.; Majidi, L. *Mater. Lett*. **2006**, 60, 2840-2843.
(30) Znini, M.; Majidi L.; Bouyanzer, A.; Paolini, J.; Desjobert, J M.; Costa J.; Hammouti, B.; *Arab. J. Chem*. **2010**, doi:10.1016/j.arabjc.2010.09.017.

(31) Afia, L.; Salghi, R.; Bammou, L.; Bazzi, El.; Hammouti, B.; Bazzi, L.; Bouyanzer, A. Journal of Saudi Chemical Society. 2011, doi:10.1016/j.jscs.2011.05.008.
(32) Znini, M.; Bouklah, M.; Majidi, L.; Kharchouf, S.; Aouniti, A.; Bouyanzer, A.; Hammouti, B.; Costa, J.; Al-Deyab, S S. *Int. J. Electrochem. Sci*. **2011**, 6, 691 – 704.
(33) Anonymous. French Pharmacopoeia. Maisonneuve S. A: Moulins-les-Metz. France. **1983**.
(34) International Standard ISO 5509 : 2000 Animal and vegetable fats and oils - Preparation of methyl esters of fatty acids. Second edition **2000**.
(35) Bouanis, F. Z.; Bentiss, F.; Traisnel, M.; Jama, C. *Electrochim. Acta*. **2009**, 54, 2371-2378.
(36) Morad, M.S.; El-Dean, A. M. K. *Corros. Sci*. **2006**, 48, 3398–3412.
(37) Tebbji, K.; Hammouti, B.; Oudda, H.; Ramdani, A.; Benkadour, M. *Appl. Surf. Sci.* **2005**, 252, 1378–1385.
(38) Yurt, A.; Balaban, A.; Ustun Kandemir, S.; Bereket, G.; Erk, B. *Mater. Chem. Phys*, **2004**, 85, 420–426.
(39) Mahdavian, M.; Ashhari, S. *Electrochim. Acta*. **2010**, 55, 1720–1724.
(40) Okafor, P. C.; Zheng, Y. *Corros. Sci*. **2009**, 51, 850–859.
(41) Lorenz, W. J.; Mansfeld, F.; Proceedings of the Sixth Symposium European Inhibition of Corrosion, University of Ferrara, Ferrara, **1985**. p. 23.
(42) Cao, C. *Corros. Sci*. **1996**, 38, 2073–2082.
(43) Bentiss, F.; Jama, C.; Mernari, B.; El Attari, H.; El Kadi, L.; Lebrini, M.; Traisnel, M.; Lagrenée, M. *Corros. Sci*. **2009**, 51, 1628-1635.
(44) McCafferty, E.; Hackerman, N *J. Electrochem. Soc*. **1972**, 119, 146-154.
(45) Li P.; Lin, J. Y.; Tan, K. L.; Lee, J. Y. *Electrochim. Acta*. **1997**, 42, 605-615.
(46) Abdel Rehim, S. S, Hazzazi, O. A.; Amin, M. A.; Khaled, K. F. *Corros. Sci*. **2008**, 50, 2258-2271.
(47) De Souza, F. S.; Spinelli, A. *Corros. Sci*. **2009**, 51, 642-649.
(48) Emreg¨ul, K. C.; Akay, A. A.; Atakol. O. *Mater. Chem. Phys*. **2005**, 93, 325-329.
(49) Bockris, J O'M.; Reddy, A K N. Modern Electrochemistry, vol. 2, Plenum Press, New York 1267. **1977**
(50) Martinez, S.; Stern, I. *Appl. Surf. Sci*. **2002**, 199, 83-89.
(51) Szauer, T.; Brand, A. *Electrochim. Acta*. **1981**, 26, 1253-1256.
(52) Guan, N M.; Xueming, L.; Fei, L. *Mater. Chem. Phys*. **2004**, 86, 59-68.
(53) Soltani, N.; Behpour, M.; Ghoreishi, S M.; Naeimi, H. *Corros. Sci*. **2010**, 52, 1351– 1361.
(54) Gomma, M K.; Wahdan, M H. *Mater. Chem. Phys*. **1995**, 39, 209–262.
(55) Sahin, M.; Bilgic, S.; Yilmaz, H. *Appl Surf Sci*. **2002**, 195, 1–7
(56) Bilgic, S.; Caliskan, N. *Appl. Surf. Sci.* **1999**, 152, 107-114.
(57) Khamis, E. *Corrosion*. **1990**, 46, 476-484.
(58) Dahmani, M.; Et-Touhami, A.; Al-Deyab, S.S.; Hammouti, B.; Bouyanzer, A. *Int. J. Electrochem. Sci*. **2010**, 5,1060-1069.
(59) Znini, M.; Majidi, L.; Laghchimi, A.; Paolini, J.; Hammouti, B.; Costa, J.; Bouyanzer, A.; Al-Deyab, S. S. *Int. J. Electrochem. Sci*. **2011**, 6, 5940-5955.
(60) Cristofari, G.; Znini, M.; Majidi, L.; Bouyanzer, A.; Paolini, J.; Hammouti, B.; Costa, J. *Int. J. Electrochem. Sci*. **2011**, 66, 699 – 671.

(2012) http://www.jmaterenvironsci.com/